

# Synchrotron IR analysis of hippocampal amyloid conformation in TgAPP2576 mice.

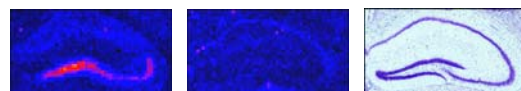
Cano, K.E.<sup>1</sup>, Nemec, J.A.<sup>1</sup>, Marinkovic, N.S.<sup>2</sup>, Sheridan, M.V.<sup>1</sup>, Linkous, D.H.<sup>1</sup>, Jones, B.F.<sup>3</sup>, & Flinn, J.M.<sup>1</sup>

1. Dept. Psychology, George Mason Univ., Fairfax, VA, USA; 2. Nat'l. Synchrotron Light Source, Brookhaven Nat'l. Lab., Upton, NY, USA; 3. Water Resources Div., U.S. Geol. Survey, Reston, VA, USA.

## Introduction

The progressive neurodegenerative disorder Alzheimer's disease (AD) is characterized by the pathological accumulation of the  $\beta$ -amyloid (A $\beta$ ) protein, which is naturally found in both soluble and insoluble forms. In its insoluble form, A $\beta$  may exist in either an  $\alpha$ -helix or a  $\beta$ -pleated sheet conformation; certain metals have been shown to alter the conformation of A $\beta$  in vitro (House et al., 2004). Previous work with microprobe synchrotron X-ray fluorescence ( $\mu$ XSRF) indicated high concentrations of certain metals in the dorsal hippocampal region of mice raised on metal-enhanced water (Linkous et al., DATE; Fig. 1). The present study examined the effects of dietary trace metals on amyloid conformation in the brains of transgenic (Tg) and wild type (WT) APP2576 mice, which develop A $\beta$  neuropathology mimicking that seen in AD.

**Figure 1:** Dorsal hippocampus in coronal sections from a Wt mouse raised on lab water. The XSRF images show zinc concentrated in the hilus (left) and iron concentrated in the CA1 region (center) of the same sample, while the cresyl violet-stain reveals structure in the adjacent tissue section (right).

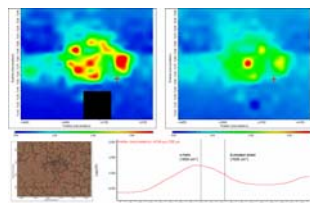


## Method

Tg(APP2576) mice expressing AD pathology and their wild-type (Wt) littermates were raised pre- and post-natally on either lab water (tap water; N=7), lab water enhanced with zinc carbonate (10ppm ZnCO<sub>3</sub>; N=12), or lab water enhanced with iron (II) nitrate (5ppm Fe(NO<sub>3</sub>)<sub>2</sub>; N=4). Lab water was regularly tested to determine the concentrations of a suite of ions, as well as pH level; metal ion levels were found to be negligible, and no significant difference was found in water consumption across water groups. At 10 months of age, animals were tested in behavioral paradigms, including Morris water maze and fear conditioning. Animals were sacrificed at 12 months of age and their brains were fresh frozen. Coronal sections of 20 $\mu$  thick-ness were taken with a Sakura Tissue-Tek Cryo3 cryostat and mounted on silver-coated low-mirrored slides (Kevley Technologies).

IR analyses were conducted using a high-powered ultraviolet synchrotron light source at Brookhaven National Laboratory (Marinkovic et al., 2002). Fourier transform infrared microscopy (FTIRM) was used to collect IR spectra. Spectra were taken from blank areas of each slide prior to tissue analysis to allow subtraction of background noise from the tissue spectra. Protein conformation was detected with OMNIC soft-ware (Thermo-Nicolet) based on peak-height intensity within the amide I band:  $\alpha$ -helix = 1650cm<sup>-1</sup>,  $\beta$ -pleated sheet = 1630cm<sup>-1</sup> (Fig. 2). OMNIC also generated false-color intensity maps, which allowed quantification of data using Image J software (National Institutes of Health) (Fig. 8).

**Figure 2:** False-color IR maps of an amyloid plaque in a Tg mouse raised on lab water. The maps show IR spectra for the point indicated by the crosshairs on the maps. You can see intensity of the  $\alpha$ -helix peak (top left) and the  $\beta$ -pleated sheet peak (top right), and the spectrum shows a line at each peak (bottom right). The plaque can be seen in the brightfield image of the tissue (bottom left). The black spot in the  $\alpha$ -helix map indicates very low intensity at that point; a glitch in the software causes the surrounding area to be blacked out in the image.



## Results

Significant differences were found in amyloid levels and conformation in areas of the dentate gyrus, with noticeable differentiation in the granule cell layer of the dentate gyrus (GrDG), which is comprised of several distinct cellular regions (Fig. 3, Fig. 4). In the hilus, zinc-treated Tg mice had significantly more  $\alpha$ -helical A $\beta$  than mice raised on lab water ( $t(17)=1.72$ ,  $p<.05$ ). There was also significantly more  $\alpha$ -helical A $\beta$  in the GrDG somas of zinc-treated Tg mice than in the GrDG somas of lab-water Tg mice ( $t(17)=1.87$ ,  $p=.03$ ). A trend was found in iron-treated mice, which displayed more  $\beta$ -pleated sheet amyloid in the hilus than did lab-water mice ( $t(9)=0.9$ ,  $p<.10$ ). ANOVA revealed differences in amyloid distribution and conformation between the GrDG and the adjacent molecular layer and hilar regions (F(1,20)=30.4,  $p<.05$ ). Overall,  $\alpha$ -helical A $\beta$  was significantly more abundant than the  $\beta$ -pleated sheet form in the GrDG, including somas, apical dendrites (ApD) and axons (F(1,25)=11.58,  $p<.01$ ), although GrDG somas had less amyloid overall than GrDG ApD or axons. Within the GrDG, somas of zinc-treated Tg mice had significantly less  $\alpha$ -helical A $\beta$  than either the ApD or axons, while lab-water Tg mice had significantly less  $\alpha$ -helical A $\beta$  in somas than in axons. The mean values for amyloid distribution in the GrDG are presented in Table 1 and Fig. 5. Analyses of  $\beta$ -pleated sheet conformation data are ongoing. Due to time limitations at the National Synchrotron Light Source, few iron Tg mice have been examined to date.

**Table 1:** Mean values for amyloid in GrDG regions. All values are for Tg mice grouped by water type.

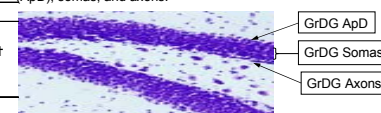
Alpha	Lab (N = 7)	Zinc (N = 12)	Iron (N = 4)
GrDG ApD	1.48 ± 1.12	1.89 ± 0.85 *	1.19 ± 0.49
GrDG Somas	0.83 ± 0.48	1.20 ± 0.37	0.94 ± 0.26 †
GrDG Axons	1.47 ± 0.80	1.58 ± 0.63 ^	1.59 ± 1.04

Beta	Lab (N = 7)	Zinc (N = 12)	Iron (N = 4)
GrDG ApD	0.96 ± 0.55	1.28 ± 0.59 *	1.31 ± 1.17
GrDG Somas	1.01 ± 0.68	1.02 ± 0.31	0.52 ± 0.32 †
GrDG Axons	1.00 ± 0.47	0.93 ± 0.36 ^	1.01 ± 0.49

\*, † Significant at  $p < 0.05$ ; ^ Significant at  $p < 0.01$

**Figure 3:** Dentate gyrus stained with cresyl violet. Labels show granule cell layer apical dendrites (ApD), somas, and axons.



**Figure 4:** Cytoarchitecture of the hippocampus (adapted from Amaral & Witter, 1995). The dentate gyrus is divided into three distinct regions: the molecular layer (ML), the granule cell layer (GCL) and the hilus (H).

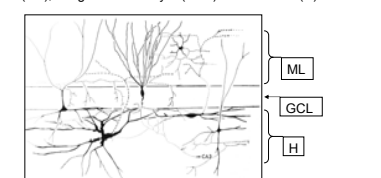


**Figure 5:** Mean values for amyloid in GrDG regions. All values are for Tg mice grouped by water type.

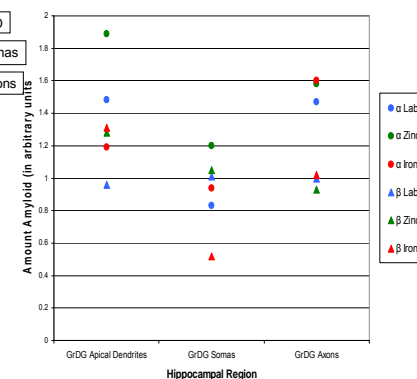
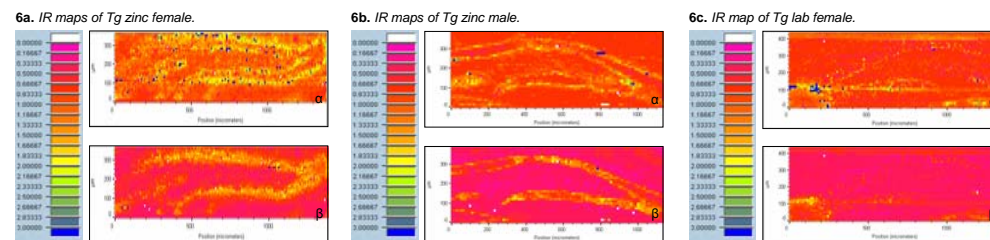


**Figure 6:** False-color intensity maps produced using OMNIC software during IR analysis. Each map shows an IR scan of the dentate gyrus region of a mouse hippocampus. The top image for each group is a map of  $\alpha$ -helix intensity. The bottom image is a map of  $\beta$ -pleated sheet intensity. Shown are scans from a Tg zinc female (6a), a Tg zinc male (6b), and a Tg lab-water female (6c). The scale-bar is a 0-3 scale showing amyloid intensity based on IR spectral values; this scale is constant across images.



## Conclusions

Previous data has shown that the administration of zinc in drinking water can impair spatial memory in rats and both Wt and Tg mice (Flinn et al., 2005). The current results show that chronic administration of enhanced dietary zinc can also change amyloid conformation, which may affect the efficacy of A $\beta$  clearance therapies. Additionally, the differences in amyloid distribution in the tissue suggest that conformational changes in amyloid may occur preferentially in certain brain regions.

## References and Acknowledgements

This study was supported by a BNL general user grant for NSLS beamline access (J.M.F.). NSLS is supported by the U.S. Department of Energy, Office of Science, Office of Basic Energy Sciences, under Contract No. DE-AC02-98CH10886.

Amaral, D.G., & Witter, M.P. (1995). Hippocampal formation. In G. Paxinos (Ed.), *The rat nervous system* (2nd Ed.) (pp. 443-493). San Diego: Academic Press.  
 Espósito, M.S., Platti, V.C., Laplagne, D.A., Morgenstern, N.A., Ferrari, C.C., Pitossi, F.J., & Schinder, A.F. (2005). Neuronal differentiation in the adult hippocampus recapitulates embryonic development. *J. Neurosci.*, 25(44): 10074-10086.  
 Flinn, J.M., Hunter, D., Linkous, D.H., Lanzrotti, A., Smith, L.N., Brightwell, J., & Jones, B.F. (2005). Enhanced dietary zinc consumption in rats causes spatial memory deficits and increased zinc levels within the brain. *Physiology and Behavior*, 83(5): 793-803.  
 House, E., Collingwood, J., Khan, A., Korzhakina, O., Berthon, G., & Exley, C. (2004). Aluminum, iron, zinc and copper influence the in vitro formation of amyloid fibrils of A $\beta$ 242 in a manner which may have consequences for metal chelation therapy in Alzheimer's disease. *J. Alz. Disease*, 6(3): 291-301.  
 Marinkovic, N. S., Huang, R., Bromberg, P., Sullivan, M., Toomey, J., Miller, L. M., Sperber, E., Moshe, S., Jones, K. W., Chouparova, E., Lappi, S., Franzen, S., and Chance, M. R. (2002). Center for Synchrotron Biosciences' U2B beamline: an international resource for biological infrared spectroscopy. *J. Synchr. Rad.*, 9: 189-197.  
 Miller, L. M., Dumas, P., Jamn, N., Teillac, J.-L., Miklossy, J., & Forro, L. (2002). Combining IR spectroscopy with fluorescence imaging in a single microscope: Biomedical applications using a synchrotron infrared source. *Rev. Sci. Instr.*, 73(3): 1357-1360.  
 Paxinos, G., & Franklin, B.J. (2000). *The mouse brain in stereotaxic coordinates: Deluxe second edition*. New York: Academic Press.